Effect of Non-axisymmetric Magnetic Perturbations on the Turbulence at Open Field Lines in ASDEX Upgrade

H.W. Müller[1], T. Eich[1], A. Kirk[2], M. Kočan[1], T. Lunt[1], C. Maszl[3],
V. Rohde[1], R. Schrittwieser[3], W. Suttrop[1], and the ASDEX Upgrade Team

[1] *Max-Planck-Institut für Plasmaphysik, EURATOM-Association, Garching, Germany*
[2] *EURATOM/UKAEA Fusion Association, Culham Science Centre, Abingdon, UK*
[3] *Inst. for Ion and Applied Physics, Univ. of Innsbruck, Association EURATOM,ÖAW, Austria*

Introduction

The impact of type-I ELMs on plasma facing components is a concern for the operation of next generation tokamaks in H-mode [1]. The possibility to influence or even to suppress ELMs by non-axisymmetric magnetic perturbation (MP) fields has been shown in several tokamaks [2, 3, 4]. Nevertheless the complex interplay of magnetic perturbations, edge currents, electric fields, plasma rotation, flows and turbulent transport is not well understood, neither in H-mode nor in L-mode.

ASDEX Upgrade [5] has been equipped with eight saddle coils mounted inside the vessel [6]. Four coils above and four below the midplane allow to create MPs of toroidal mode numbers up to n=2 in even and odd parity. This coil set is able to mitigate ELMs in ASDEX Upgrade above a certain edge density threshold. ELM mitigation does not depend on the resonance of the applied MPs [7].

In this paper the influence of non-axisymmetric MPs on turbulence in the scrape-off layer (SOL) is investigated in L-mode and H-mode by means of a reciprocating probe (RCP). The probe was equipped with a multi-pin probe head carrying ten in-plane tips in a Mach probe arrangement. On each side of the Mach probe there are five poloidally staggered tips [8]. The probe head is tilted with respect to the equatorial plane in such way that the pin pairs for flow measurements are aligned to the inclined magnetic field and the poloidally staggered pins are perpendicular to the field. All presented measurements were done with the Langmuir pins connected towards the inner divertor.

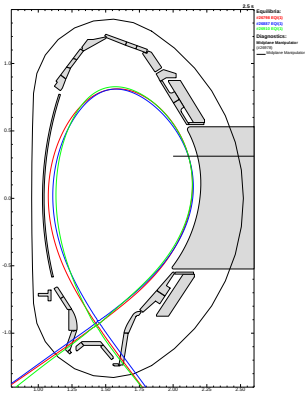

Figure 1: *Poloidal cross section of ASDEX Upgrade and location of reciprocating probe with plasma shapes used in L-mode (red and blue) and H-mode (green) discharges.*

Observations in L-mode

The investigations in L-mode have been performed in lower single null (LSN) discharges with the ion drift direction towards the active divertor. The discharges had a plasma current $I_p = 1.0\,\mathrm{MA}$, a toroidal magnetic field $B_t = -2.5\,\mathrm{T}$ and additional heating power by ECRH $P_{ECRH} = 640\,\mathrm{kW}$. The line averaged density $\bar{n}_e$ was varied from 1.5 to $4.6 \times 10^{19}\,\mathrm{m}^{-3}$ from shot to shot. The two plasma shapes used for the L-mode discharges are shown in figure 1. The perturbation coils were operated in the second part of the discharges with odd configuration and a toroidal mode number of n=2. $\bar{n}_e$ was feedback controlled. The required neutral gas flux was approximately constant throughout the discharge indicating that neither density pump out nor

density rise occurred when switching on the MPs. Also the energy content and total radiation P_{rad} were not influenced by the MPs despite some reduction in P_{rad} for the lowest densities.

With increasing current the MP coils first cause localized radial wiggles [9] before the islands overlap and stochastic behaviour occurs. In this process finger-like magnetic structures form around the X-point [10] leading to strikeline splitting [11] which is an indication of the formation of ergodic layers. At ASDEX Upgrade only for low densities in the range $1.5-2.2\times10^{19}\,\mathrm{m}^{-3}$ strikeline splitting was found in L-mode but not for $\bar{n}_e \geq 3\times10^{19}\,\mathrm{m}^{-3}$. With ergodization flux surfaces could be destroyed and no separatrix in the classical sense might exist. For the comparison of SOL data with and without MPs a reference point equivalent to the separatrix is required. The magnetic reconstruction delivers a radial inward shift of the separatrix by $\Delta R_{sep} = 3-5\,\mathrm{mm}$ at the poloidal position of the RCP when the MPs are switched on. But the magnetic measurements and the RCP are toroidally separated. At the poloidal RCP position the radial deviation of R_{sep} is $\pm5\,\mathrm{mm}$ around the torus [9]. Cross correlation of two poloidally staggered Langmuir pins allows measuring the velocity perpendicular to the magnetic field $v_\perp$. Close to the separatrix a change in the $v_\perp$ direction from the ion to electron drift direction occurs [12]. This shear layer can be used to benchmark a separatrix-equivalent position even when the flux surface structure is destroyed. In # 26887 ($\bar{n}_e = 4.6\times10^{19}\,\mathrm{m}^{-3}$) the RCP probe reached the shear layer in both periods, with and without MPs. The magnetic reconstruction delivered a radial inward shift $\Delta R_{sep} = 3-4\,\mathrm{mm}$ with the MPs on. The same shift occurs for the shear layer. The shear layer is accompanied by a steepening of the floating potential (V_{flt}). In the low density discharges the shear layer was hit only when the coils were off. Here the gradient steepening is used as additional information to determine a separatrix-equivalent position. In # 26798 ($\bar{n}_e = 1.5\times10^{19}\,\mathrm{m}^{-3}$) the equilibrium reconstruction determines a $\Delta R_{sep} = 3-5\,\mathrm{mm}$. From the position of the shear layer and the steepening of the V_{flt} profile a similar shift of about $5-6\,\mathrm{mm}$ is deduced.

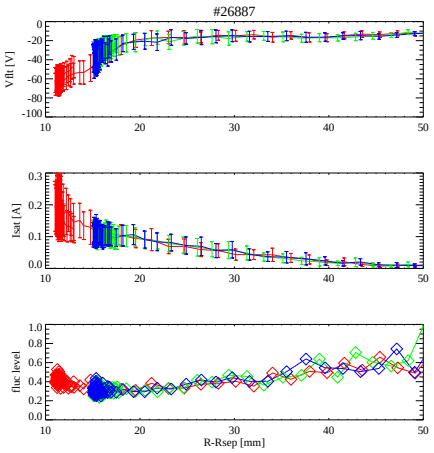

Figure 2: *V_{flt}, I_{sat} and $\delta I_{sat}/I_{sat}$ profiles over distance to separatrix $R-R_{sep}$ for a high density L-mode.*

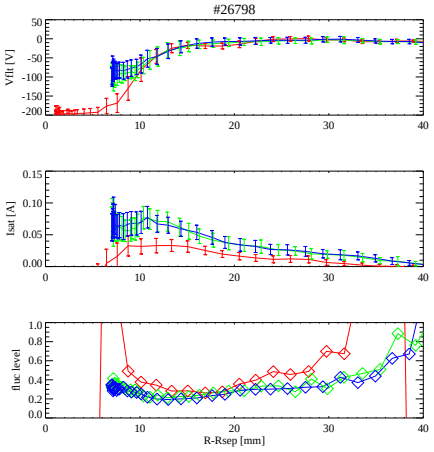

Figure 3: *V_{flt}, I_{sat} and $\delta I_{sat}/I_{sat}$ profiles over distance to separatrix $R-R_{sep}$ for a low density L-mode.*

In discharge # 26887, $\bar{n}_e = 4.6\times10^{19}\,\mathrm{m}^{-3}$, the infrared camera observing the inner divertor detected no strikeline splitting. The V_{flt} profiles, the ion saturation current I_{sat} and the relative fluctuation level $\delta I_{sat}/I_{sat}$ (δI_{sat} is the standard deviation of I_{sat}) are shown in figure 2 for the reference case with coils off in red and coils on in green and blue. The profiles with MPs are shifted

by 4 mm outward as discussed in the previous paragraph. Also with $\bar{n}_e = 3 \times 10^{19}\,\mathrm{m}^{-3}$ there is no strikeline splitting visible. In # 26798 with the density lowered to $\bar{n}_e = 1.5 \times 10^{19}\,\mathrm{m}^{-3}$, strikeline splitting occurred and the profiles with and without MPs show significant differences, figure 3 (red: reference case, blue and green: coils on). The gradient of the floating potential becomes flatter with the MPs while I_{sat} (dominated by the electron density) rises by a factor of two for $R - R_{sep} > 10\,\mathrm{mm}$. Closer to the separatrix the I_{sat} measurements become critical (MP case) or even break down (reference case) since the floating potential reaches 50% of the bias voltage ($-190\,\mathrm{V}$). In the reference case also V_{flt} is underestimated for $R - R_{sep} < 6\,\mathrm{mm}$ due to the data acquisition limited to $\pm 200\,\mathrm{V}$. Depending on $R - R_{sep}$ the fluctuation level with coils is $50 - 100\%$ of $\delta I_{sat}/I_{sat}$ without coils. The behaviour of I_{sat} in the SOL and the flattening of the V_{flt} gradient agrees with observations at MAST [13]. For $\bar{n}_e = 2.3 \times 10^{19}\,\mathrm{m}^{-3}$ the infrared camera still detected a weak strikeline splitting at the inner divertor. For $R - R_{sep} < 40\,\mathrm{mm}$ the probe measurements in the SOL show a lowering of V_{flt} by about 10 V. For I_{sat} there might be a slight increase but this is uncertain within the error bars.

Observations in H-mode

A series of discharges was performed in H-mode to study the influence of the MPs on ELMs. All discharges were run in the same way despite the settings of the perturbation coils. The LSN discharge parameter were $I_p = 0.8\,\mathrm{MA}$, $B_t = -2.5\,\mathrm{T}$, neutral beam heating power $P_{NBI} = 7.5\,\mathrm{MW}$, $P_{ECRH} = 2\,\mathrm{MW}$. Until 3.4 s the line averaged density was about $\bar{n}_e = 6.5 \times 10^{19}\,\mathrm{m}^{-3}$ then ramped up to $\bar{n}_e = 7.3 \times 10^{19}\,\mathrm{m}^{-3}$ at 4 s. The MPs, n=2, odd parity, were switched on at 1.9 s and off at 5.6 s. Until the increase of $\bar{n}_e$ the edge density is below the threshold for ELM mitigation [7]. At higher density the ELMs are mitigated but not fully suppressed as can be seen in figure 5 on the left hand side. The full mitigation is achieved at 4.0 s. During the low density phase, independent if the coils are off or on, large type-I ELMs appear with $f_{ELM} = 30 - 70\,\mathrm{Hz}$ and an energy loss of typically $dW_{mhd} = 30 - 70\,\mathrm{kJ}$. Smaller ones show up in between the large ones. In the ELM-mitigated period the ELMs occur with $f_{ELM} = 100 - 300\,\mathrm{Hz}$ and $dW_{mhd} = 0 - 10\,\mathrm{kJ}$.

In each discharge four reciprocations were performed ($t = 1.5, 2.6, 3.9, 5.5\,\mathrm{s}$) to measure the reference and perturbed case for both densities. The last strokes are skipped here since several parameters changed at once not allowing to study the influence of the MPs. From # 26910 to # 26911 the MP field was turned by 90° toroidally. This allows reconstructing the mean separatrix position by comparison of the I_{sat} profiles in the two MP field configurations and with and without MPs [9]. A correction of $R_{sep} = \pm 3\,\mathrm{mm}$ has to be applied for the toroidal non-symmetric effects.With these corrections the I_{sat} profiles can be compared. An example is shown in figure 4 where large ELMs were cut out. Since the error bars are rather

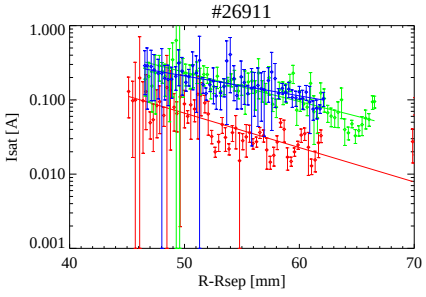

Figure 4: *I_{sat} profiles without MPs (red), with MP but without ELM mitigation (green) and ELM-mitigated period (blue). The solid lines indicate exponential fits to the profiles.*

large and some influence by limiters cannot be ruled out
a quantitative analysis cannot be done. It seems to be robust that the I_{sat} level and the fall-off length rise in the far SOL with the MPs switched on. With the MPs the profile of the ELM mitigation phase is very close to the profile at lower $\bar{n}_e$ without ELM mitigation.

Three periods of # 26911 while the probe was at $R - R_{sep} = 45 - 48$ mm are compared in figure 5. At $t = 1.616, 2.701, 4.016$ s time slices of 20 ms have been cut out corresponding to the reference case (red), the periods with MPs at lower density (green) and higher density with ELM mitigation (blue). $I_{polsoli}$ is the shunt current of the inner divertor tiles which reflects the electron temperature in the divertor and acts as an ELM monitor. Well visible are the type-I ELMs in the first two periods while during the ELM-mitigated phase only weak oscillations occur in agreement with the variations in W_{mhd}. The base level of I_{sat} rises twice - with switching on the MPs and with the onset of the ELM mitigation at higher $\bar{n}_e$. The type-I ELMs are related to strong I_{sat} oscillations with peak values of $2-3$ A. In between there are smaller spikes related to smaller transport events. Unexpected are the large I_{sat} peaks(> 2 A) in the ELM-mitigated phase. The I_{sat} bursts are related to the small $I_{polsoli}$ peaks in the divertor. These bursts cannot carry much energy. The I_{sat} mean value for the time window shown rises by about a factor of 2 with the MPs while δI_{sat} stays unchanged all time. Looking at the normalized PDF of I_{sat} where the x-axis is normalized to the standard deviation it is obvious that the PDFs for both periods with MPs are the same showing a skewness of 3.0 while it is 6.3 in the reference case indicating a less filamentary transport with MPs in the far SOL.

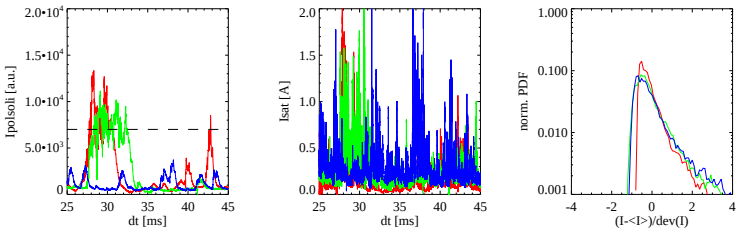

Figure 5: *Time traces of $I_{polsoli}$, I_{sat} and the according normalized PDF for three periods (MP off (red), MP on with (blue) and without ELM mitigation (green)) in # 26911. The broken line indicates the level of large ELMs.*

References

[1] A. Loarte et al., Plasma Phys. Control. Fusion **45**, 1549 (2003)
[2] T.C. Hender et al., Nucl. Fusion **32**, 2091 (1992)
[3] Y. Liang et al., Phys. Rev. Lett. **98**, 265004 (2003)
[4] T. Evans et al., Phys. Rev. Lett. **92**, 235003 (2004)
[5] A. Herrmann, O.Gruber, Fusion Sci. Technol. **44**, 569 (2003)
[6] W. Suttrop et al., Fus. Eng. Design **84**, 290 (2009)
[7] W. Suttrop et al., Phys. Rev. Lett. **106**, 225004 (2011)
[8] H.W. Müller et al., Contr. Plasma Phys. **50**, 847 (2010)
[9] J.C. Fuchs et al., this conference
[10] R.K.W. Röder et al., Phys. Plasmas **10**, 3796 (2003)
[11] T. Eich et al., Nucl. Fusion **40**, 1757 (2010)
[12] B. Nold et al., Plasma Phys. Control. Fusion **52** 065005 (2010)
[13] P. Tamain et al., Plasma Phys. Control. Fusion **52** 075017 (2010)